A Physically-Based Model for Oxidation in a Circular Trench in Silicon

Y. Xu, C. Sudhama, S. Hong, J. A. Sellers, S. Ambadi, K. Kamekona, G. Averett, B. Ruiz, I. Wan, W. Cai, Y. Wu, J. C. Costa and R. B. Davies*

ON Semiconductor, Maildrop AE100, 5005 E. McDowell Road, Phoenix, AZ 85008
Phone: 602-244-3660 c.sudhama@onsemi.com

*Advanced Device Design, Inc., 433 E. McKinley St., Tempe, AZ 85281

ABSTRACT

Oxidation in a circular trench is of relevance in several applications, including trench capacitors in memories. In this work a model for stress-dependent oxidation is presented. The model is based on modifications of the Deal-Grove model, which is used conventionally for planar oxidation. It is seen that even when stress-effects are ignored, the circular trench geometry leads to a drop in the oxidation rate, in comparison to planar oxidation. The oxidation rate drops even further as the initial diameter of the trench is reduced. When the stress due to volume-expansion is included, with silicon dioxide considered as an elastic material, an additional drop is seen in the oxidation rate. Calibration of the model to measured data involves only a few parameters. Experimental data are presented that qualitatively demonstrate some predictions of the theory.

Keywords: circular, trench, convex, concave, wet, dry, oxidation, Deal-Grove, stress-dependence, retardation.

1 INTRODUCTION

In modern IC technology, trenches have many applications, such as device-isolation and substrate contact formation. Trenches are usually two-dimensional, meaning that while they have the well-known 2-D cross-section, in the third dimension they are relatively long. The simulation of oxidation in such structures is relatively simple, as illustrated in Fig. 1. Circular, square and oval trenches also have technological importance in various applications, including trench-capacitors, where the capacitance-per-unit-area is improved by extending the trench deep into the silicon substrate [1-2], and in certain dielectric isolation structures. The process-simulation of such trenches necessarily requires 3-D meshes and the appropriate numerics in the code. Considering the state of the art of commercially available process simulators, simulating trenches in 3-D is difficult at best.

A computationally inexpensive alternative for estimating oxidation rates in circular trenches may be to discard 3-D effects occurring at the concave bottoms and convex tops of the trenches, and focus on the quasi-2-D regions of the cylindrical cross-sections, far away from the bottom and top. This can certainly be accomplished in a commercially-available 2-D simulator. In order to gain physical insight into the mechanisms involved, however, it is valuable to also pursue analytical solutions to the 2-D problem of stress-dependent oxidation in a circular trench. Previous work in this field includes that of D.-B. Kao, et al [4-5]. Our approach differs in certain important ways, as highlighted in the sections below.

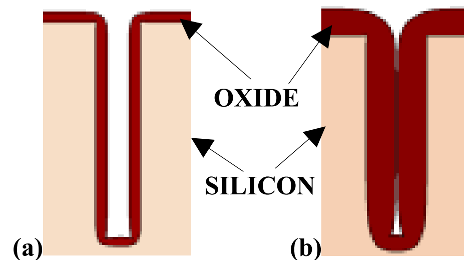

Fig. 1. Cross-sections from the 2-D simulation of oxidation in a long trench (a) early in the process, and (b) close to the natural end-point of the process. Here the trench is considered to be infinitely long in the third dimension. 2-D effects at the concave corners of the bottom and convex corners of the top of the trench are easily captured in ISE-DIOS [3].

2 A GEOMETRICAL CONSTRAINT

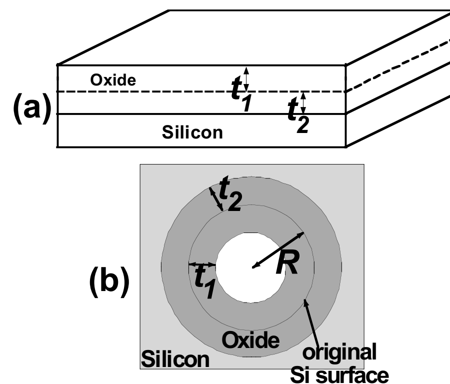

Fig. 2. Schematic for (a) planar oxidation, where t_1=(14/11)t_2 and (b) for the circular trench. R is the initial trench radius and t_2 is the thickness of silicon consumed.

As shown in Fig. 2(a), for planar oxidation the formation of a layer of silicon dioxide (100% volume) occurs through the consumption of 44% of silicon (by volume). In Fig. 2(b) the 2-D cross-section of a circular trench is shown. Here R is the radius of the trench before oxidation, t_2 is the thickness of silicon consumed and $t_1 + t_2$ is the thickness of the oxide formed. Assuming the same volumetric expansion in the circular case as in the planar, for a given t_2 (i.e., for a given thickness of consumed silicon) it can be shown that

$$t_1 = R - R\sqrt{1-\frac{14}{11}\left(\left(\frac{t_2}{R}\right)^2+\frac{2t_2}{R}\right)} . \quad (1)$$

An important feature of oxidation in a circular trench is that the process is self-limiting: when the grown oxide fills the trench, oxidation can no longer occur. When this happens, $t_{1,max}=R$, and therefore from Eq. 1, $1-\frac{14}{11}\left(\left(\frac{t_{2,\max}}{R}\right)^2+\frac{2t_{2,\max}}{R}\right)=0$. From this it is easy to see that:

$$(t_1 + t_2)_{\max} = R\sqrt{25/14} = 1.34R . \quad (2)$$

Additionally, using a Taylor series expansion of Eq. 1, and ignoring higher order terms in R, it is seen that

$$t_1 \approx \frac{14}{11}t_2 + \frac{7}{11}\frac{t_2^2}{R} , \quad (3)$$

which, when compared to the relation for the one-dimensional (planar) case: $t_1=(14/11)t_2$, suggests that *for a fixed thickness of consumed silicon*, the oxide grown in the circular trench is thicker than in the planar case. This is an intuitively satisfying result. It must be mentioned that in order to consume the same thickness of silicon in the planar and circular cases, different oxidation recipes are necessary. This is due to the retardation of oxidation in the circular trench, as explained in the following sections.

3 THE STRESS-FREE MODEL

The stress-free solution to the diffusion equations for the planar (1-D) case is after Deal and Grove, as in [6]. In that analysis, $F_1=h(C^*-C_o)$ is the incident oxidant flux on the oxide surface, $F_2=D((C_o-C_i)/x)$ is the flux due to diffusion inside the oxide, and $F_3=k_sC_i$ is the flux incident on the Si/SiO$_2$ interface. Here h is the mass transfer coefficient for oxidant atoms, C^* is the equilibrium concentration (solubility limit) of oxidants in oxide, C_o is the concentration on the oxide surface and C_i is the concentration at the Si/SiO$_2$ interface. Also, k_s is the reaction rate constant at the interface, D is the diffusivity of oxidants in the oxide and x is the spatial coordinate. In the 1-D case, $F_1=F_2=F_3$, and the following equation:

$$N_1\frac{dx}{dt}=\frac{k_sC^*}{1+k_s/h+k_sx/D}, \quad (4)$$

is solved exactly to derive the growth equation, where N_1 is $2.2x10^{22}\mu m^{-3}$ for dry oxidation and $4.4x10^{22}\mu m^{-3}$ for steam. The solution is plotted in Fig. 4.

A similar analysis can be performed for the circular case. In reality the growth of oxide in a circular trench is dependent on stress and possibly also on crystal orientation. In this section, the analysis will ignore stress- as well as orientation-effects. As a result one can assume radial symmetry, which simplifies the analysis.

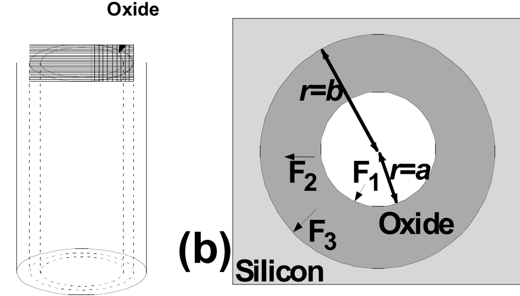

Fig. 3. Schematic cross-section of the circular trench showing the coordinate axes and the various oxidant fluxes involved.

As shown in Fig. 3, at some point during the growth of oxide in a trench, the radial coordinate is r, such that $r=a$ for the oxide surface and $r=b$ for the interface. For steady state diffusion, it can be shown that

$$\frac{1}{r}\frac{\partial C}{\partial r}+\frac{\partial^2 C}{\partial r^2}=0 \text{ or } \frac{1}{r^2}\frac{\partial}{\partial r}\left(r\frac{\partial C}{\partial r}\right)=0, \quad (5)$$

such that $C=C_o$ for $r=a$ and $C=C_i$ for $r=b$. The solution to Eq. 5 is easily obtained:

$$C = C_o + \frac{C_o-C_i}{\ln(b/a)}\ln\frac{a}{r} \quad (6)$$

into which the boundary conditions for $r=a$ and $r=b$ can be applied, to obtain $F_2=\frac{C_o-C_i}{\ln(b/a)}\frac{D}{a}$ and $F_3=\frac{C_o-C_i}{\ln(b/a)}\frac{D}{b}$, such that $F_2/F_3=b/a$. The governing equation therefore becomes:

$$N_1\frac{dx}{dt}=\frac{k_sC^*}{\left(1+\frac{k_s}{h}\frac{b}{a}\right)+\frac{k_s}{D}b.\ln\frac{b}{a}}. \quad (7)$$

An analytical solution to Eq. 7 does not exist, which is why a numerical solution is sought using the Runge-Kutta method [7]. When dry-oxidation is chosen, the constants take the following values: $N_1=2.2x10^{10}\mu m^{-3}$, $k_s=3.0x10^4\mu m/hr$, $h=3x10^7\mu m/hr$, $D=2.48x10^3\mu m^2/hr$ and $C^*=5.2x10^4\mu m^{-3}$. From these assumptions, a growth rate can be numerically solved for. It is also plotted in Fig. 4.

Note that *even when stress-effects are neglected*, there is a retardation of oxidation in the circular trench, simply due to the 2-D spreading of the oxidant flux. This point is important, but has not been emphasized in [4-5]. Another (obvious) effect of the spreading flux is the dependence of oxidation rate on the initial diameter of the trench in silicon.

As shown in Fig. 4, the smaller the trench is, the smaller is the simulated growth rate. The flattening of the growth curve occurs at the point where the trench is filled with oxide and oxidant atoms can no longer enter the interior of the trench to cause further oxidation. There is good agreement between Fig. 4 and Eq. 2.

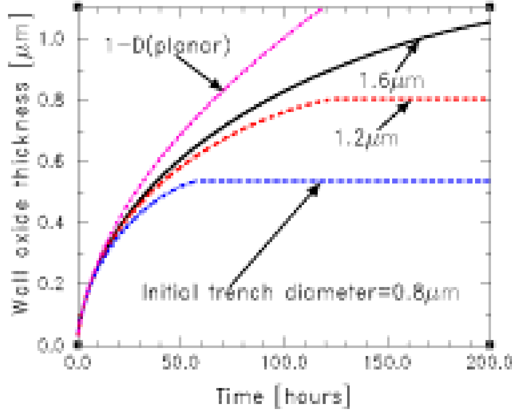

Fig. 4. Dry oxidation thickness as a function of time for a circular trench for various initial trench diameters. The growth curve for stress-free planar (1-D) oxidation is also shown for comparison. The curves for the smaller trenches flatten because the trenches are filled with oxide and no further oxidation is possible.

In this section only dry oxidation has been considered, but with changed values for constants, the equations apply to wet oxidation as well.

4 THE INCLUSION OF STRESS

Our initial experiments of wet-oxidation in circular trenches involved long oxidation times, which resulted in so much stress that the wafers were too warped to be handled by vacuum wands in the factory. ANSYS [8] simulations indicate that a mismatch in the coefficient of thermal expansion between Si and SiO_2 is unable to explain this warping. Instead, we attribute the high stress associated with trench oxidation to the volume expansion occurring during silicon oxidation: in the circular trench, the growing oxide experiences a restraint on its expansion. This restraint leads to stress and also gets stronger as oxidation proceeds.

Previous work in this area [4-5] assumed a viscous model for the oxide, and a fluid-mechanic origin for stress. In the present paper we instead assume an elastic nature for the oxide, which is perhaps more realistic. A viscoelastic model is possibly more sophisticated, but is also more difficult from the analytical viewpoint.

The introduction of stress into the growth equations is simply through the modification of k_s, the interfacial reaction rate, and of D, the diffusion coefficient, as in [3]. This is clearly a phenomenological approach, but has the virtue of being simple. (Since crystal-orientation effects are neglected in this analysis, growth-rate and stress are again dependent on radial position alone). As a result of stress one may assume the following Arrhenius relations for the reaction rate and diffusivity:

$$K_s(\sigma_n, T) = K_{so}[\,\min(1, \exp(\frac{\sigma_n V_K}{kT}))] \text{, and}$$

$$D(P,T) = D_o[\,\min(1, \exp(-\frac{P V_D}{kT}))] \quad (8)$$

where σ_n is the normal stress at the Si/SiO_2 interface, and P is the pressure at the interface.

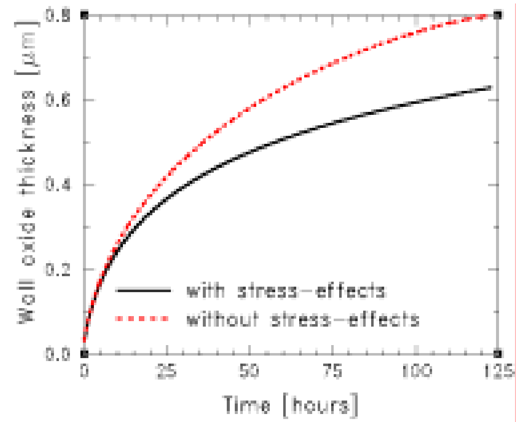

Fig. 5. The effect of elastic (volume-expansion related) stress on the oxidation rate in a circular trench with an initial diameter of *1.2μm*. The characteristic volumes V_D and V_K (Eq. 8-10) may be used to calibrate the model to measured data.

An important aspect of our stress model is the calculation of radial pressure arising from elastic stress. In the cylindrical polar coordinate system, we consider two domains, namely the growing oxide and the silicon region. By considering an Airy stress function, and applying the *natural* and *continuity* boundary conditions, it can be shown through an involved analysis that:

$$P = -\frac{1}{3}(\sigma_{rr} + \sigma_{\theta\theta} + \sigma_{zz}) = -\frac{(1+\nu_{SiO2})}{3}(\sigma_{rr} + \sigma_{\theta\theta}), \quad (9)$$

where **[σ]** is the 3-D stress tensor, r, _ and z are the cylidrical polar coordinates, and ν is Poisson's ratio. From Eq. 9 the following may be derived:

$$P = -\frac{4(1+\nu_{SiO2})}{3}\frac{S_3/S_1}{S_2/S_1 - 2a^2}, \quad (10)$$

where

$$S_1 = -\frac{(1+\nu_{SiO2})}{b.E_{SiO2}} + \frac{(1+\nu_{Si})}{b.E_{Si}},\; S_2 = \frac{2(1-\nu_{SiO2})b}{E_{SiO2}} + \frac{2(1+\nu_{Si})b}{E_{Si}},$$

and S_3=_bt_1/t_2, where E is Young's modulus, t_1 and t_2 are shown in Fig. 2, and a and b are as in Fig. 3. The stress and pressure calculated in this way are found to be compressive.

As Fig. 5 shows, there is a significant impact of stress on the oxidation rates. Here, V_D, V_K, ν and E may be used to calibrate the model to experimental data.

5 EXPERIMENTAL RESULTS

Trench oxidation experiments involved the etching of *3µm* and *10µm* deep trenches in silicon, with trench diameters ranging from *0.8µm* to *1.6µm*. This was followed by oxidation, with the planar (nominal) oxide thickness ranging from *0.1µm* to *1.0µm*. Fig. 6(a) shows the plan view of a trench prior to oxidation, while Fig. 6(b) shows an example of a trench cross-section after oxidation. It is clear that the thickness of oxide is lower on the trench walls than on the planar surface next to the trench. As explained in the previous sections, this is the result of geometry and stress effects during oxidation. In Fig. 6(b), stress-induced cracks in the silicon are also clearly visible.

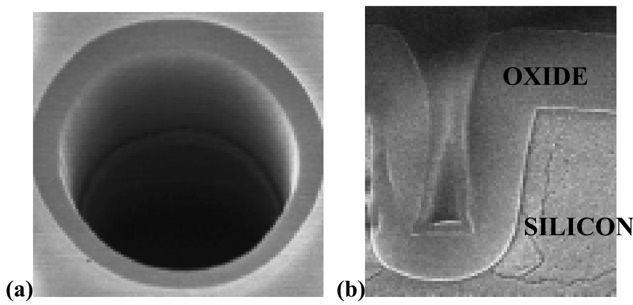

Fig. 6. (a) Plan-view SEM of a circular trench with a *~1µm* diameter. (b) Cross-sectional SEM image of the *~3µm* deep trench. The sidewall oxide is visibly thinner than the oxide in the planar region, due to geometry and stress effects. The planar oxide thickness is *~1µm*.

Fig. 7 shows measured oxide thicknesses in a circular trench, as a function of initial trench radius, for different nominal oxide thicknesses. In the *100nm* case the retardation is negligible, but is clearly present for the *300nm* case and even more prominent for the *1.1µm* case. Furthermore, the dependence on initial trench radius is negligible in the *100nm* case, but is apparent for the *300nm* case. The small dependence for these cases is consistent with the prediction in Fig. 4. Due to uncertainties introduced by the SEM measurements and due to the incompleteness of the data, model-calibration is not attempted here. Additional experiments and analysis are underway and will be reported separately.

6 CONCLUSIONS

A model has been developed for 2-D oxidation on walls of circular trenches. Even in the stress-free case, geometry effects cause a retardation of oxidation. Stress, understood to be due to volume expansion in elastic SiO_2, causes a further retardation in the oxidation. Experimental data indicate that for a trench with a diameter in the *1µm* range, retardation effects are visible at or beyond *300nm* of oxidation. Additional experimental data are needed for calibrating the theoretical model.

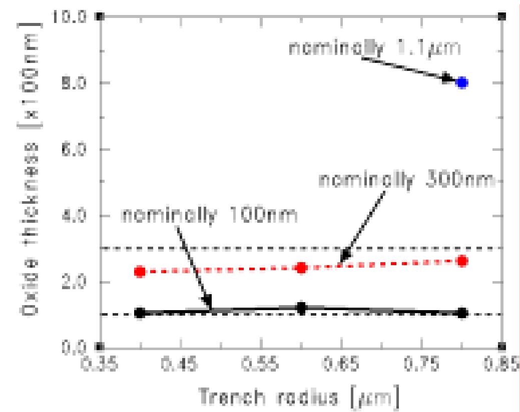

Fig. 7. Oxide thickness versus trench radius, for various recipes. In the *100nm* case, there is essentially no retardation and no variation with initial radius. For the *300nm* case, the thickness is consistently less than the nominal value; the dependence on initial trench radius is visible, but not significant, consistent with Fig. 4. In the *1.1µm* case there is a significant drop in thickness in comparison to the 1-D situation. These data were obtained from *10µm* deep trenches, wherein there is no ambiguity in the oxide thickness measurement.

ACKNOWLEDGEMENTS

We thank Al Merino, Elaine Paull, Rob Watkins & Hien Nguyen for high-quality SEM images, Roger Stout for helpful discussions, and Frank Carney for supporting this work.

REFERENCES

[1] C. J. Radens, et al, IEEE-IEDM Tech. Dig., 2000, #15-1

[2] T. Kajiyama, et al, IEEE-IEDM Tech. Dig., 2000, #15-3.

[3] DIOS, Integrated Systems Eng., http://www.ise.com/

[4] D-B. Kao, et al, IEEE-Trans. on Elec. Dev., May 1987, p1008-1017.

[5] D-B. Kao, et al, IEEE-Trans. on Elec. Dev., January 1988, p25-37.

[6] *Silicon Processing for the VLSI Era, Vol. 1*, S. Wolf & R. N. Tauber, Lattice Press, 1986, p. 198-241.

[7] *Numerical Methods for ODEs*, 2nd Edition, Daniel Zwillinger, Academic Press, Inc, 1992, p. 684-686.

[8] Swanson Analysis System, Inc., http://www.ansys.com/